Positron Deposition in Plasmas by Positronium Beam Ionization and Transport of Positrons in Tokamak Plasmas

PPPL--2392

DE87 005627

T. J. Murphy

Plasma Physics Laboratory, Princeton University

Princeton, New Jersey 08544

Abstract

The deposition of positrons from the passage of a positronium beam through a tokamak plasma and the subsequent radial transport of positrons to the limiter are simulated. The signal created by the annihilation of positrons at the limiter is calculated for several different transport models. Loss processes, such as reformation of positronium and annihilation of positrons by plasma electrons, are examined to determine how they affect the annihilation signal. An analysis of how quantities relevant to electron-mass particle transport can be obtained from a positron transport experiment is included.

I. INTRODUCTION

In a recently proposed positron transport experiment,[1] positrons would be deposited in a fusion plasma by forming a positronium (Ps) beam and passing it through the plasma. Positrons would be deposited as the beam is ionized by plasma ions and electrons. Radial transport of the positrons to the limiter could then be measured by detecting the gamma radiation produced by annihilation of positrons with electrons in the limiter. This would allow measurements of the transport of electron-mass particles and might shed some light on the mechanisms of electron transport in fusion plasmas.

In this paper, the deposition and transport of positrons in a tokamak are simulated and the annihilation signal determined for several transport models. Calculations of the expected signals are necessary for the optimal design of a positron transport experiment.

There are several mechanisms for the loss of positrons besides transport to the limiter. Annihilation with plasma electrons and reformation of positronium in positron-hydrogen collisions are two such processes. These processes can alter the signal and place restrictions on the plasma conditions in which positron transport experiments can be effectively performed.

II. DEPOSITION

A. Physics

In order to inject positrons into a magnetized plasma, they must first be neutralized, otherwise the magnetic field of the containment device will pre-

vent them from reaching the plasma. This neutralization can be accomplished by sending the positron beam through a thin carbon film.[2] One-fourth of the positronium formed will be in the $J = 0$ state (p-Ps) and will have an annihilation lifetime of 0.125 ns.[3,4] Three-fourths will be in the $J = 1$ state (o-Ps) which, in the absence of a magnetic field, has a much longer lifetime of 142 ns. The addition of a magnetic field causes the $J = 0$, $m_J = 0$ state and the $J = 1$, $m_J = 0$ state to mix and results in a drastic decrease in the lifetime of the $J = 1$, $m_J = 0$ state.[5] The lifetime of the $J = 1$, $m_J = \pm 1$ states is not affected by the magnetic field. The much greater lifetime of these states allows a significant fraction of the positronium beam to survive the distance from the foil to the plasma to be ionized and deposited as positrons.

Besides annihilation, another positronium loss mechanism is the conversion of o-Ps to p-Ps through collisions with free electrons[6] or hydrogen atoms.[7] When the o-Ps is converted to p-Ps, its lifetime is greatly reduced, and for the plasma density regimes of interest, the p-Ps will annihilate long before it has a chance to be ionized. One paper[8] reports a rather large value for the cross section for o-p conversion of positronium, but this result has been discounted[9] since it uses first order perturbation theory for electron energies near zero and disagrees with a much more rigorous approach.[6] The cross section for o-p conversion by electrons was calculated from the partial-wave phase shifts[6] using the expression[9]

$$\sigma_c = \frac{\pi a_o^2}{4k^2} \sum_\ell (2\ell - 1) \sin^2(\delta_\ell^s - \delta_\ell^t) \qquad (1)$$

and is shown in Fig. 1. The o-p conversion cross section for impact on hydrogen atoms is shown in Fig. 2.

As the positronium beam passes through the plasma, a certain fraction of

the positronium atoms are ionized yielding free positrons. Five processes for ionization are taken into account:

$$\begin{aligned} \mathrm{Ps} + \mathrm{p} &\longrightarrow e^+ + e^- + \mathrm{p} \\ &\longrightarrow e^+ + \mathrm{H} \\ \mathrm{Ps} + \mathrm{I}^{+Z} &\longrightarrow e^+ + e^- + \mathrm{I}^{+Z} \\ &\longrightarrow e^+ + \mathrm{I}^{+(Z-1)} \\ \mathrm{Ps} + e^- &\longrightarrow e^+ + e^- + e^-, \end{aligned} \tag{2}$$

where I^{+Z} is a fully stripped impurity ion and $\mathrm{I}^{+(Z-1)}$ is a hydrogen-like impurity ion. The cross sections for the Ps + p reactions (Fig. 3) were interpolated from cross sections supplied by R. Olson.[10] They were calculated numerically as a classical three-dimensional three-body problem.

Ionization by impurity ions can be taken into account by defining σ_{eff}.

$$n_e \sigma_{eff} \equiv \sum_i n_i \sigma_i, \tag{3}$$

where n_i is the density of each ion species and σ_i is the ionization cross section for that species. The cross section for each impurity is roughly proportional to the charge[11] of the impurity ion, Z_i, so

$$\begin{aligned} n_e \sigma_{eff} &\simeq \sum_i n_i (Z_i \sigma_H) \\ &\simeq n_e \sigma_H, \end{aligned} \tag{4}$$

where σ_H is the cross section for ionization by protons. Thus, the impurities may be taken into account by using the electron density instead of the ion density and using the cross section for hydrogen. This is equivalent to assuming that the plasma is pure hydrogen.

The cross section for ionization by electrons was derived by modifying the Gryziński expression[12] for the ionization of hydrogen by electron impact. The Gryziński cross section is given by

$$\sigma = \frac{\sigma_o}{U_i^2} g_i(x), \tag{5}$$

where

$$\begin{aligned} \sigma_o &= \pi e^4 = 6.52 \times 10^{-14}\,\mathrm{eV^2\,cm^2} \\ x &= \frac{E}{U_i} \\ g_i(x) &= \frac{1}{x}\left(\frac{x-1}{x+1}\right)^{3/2}\left[1 + \frac{2}{3}\left(1 - \frac{1}{2x}\right)\ln\left(2.7 + \sqrt{x-1}\right)\right], \end{aligned}$$

and where E is the electron energy and U_i is the ionization potential. This expression gives the cross section for collisions which leave the electron in the hydrogen atom with enough energy to escape from the hydrogen atom.

Three modifications are necessary to make the Gryziński expression valid for positronium. Since the ionization potential of Ps is half that of hydrogen, this lower value must be used for U_i. Since half of the energy given to the electron in the positronium atom is taken in the recoil of the Ps center of mass, any occurrence of U_i in the expression must be replaced by $2U_i$. Finally, since the plasma electrons can scatter either the electron or positron in the positronium, the cross section must be doubled. The final result is that the cross section for ionization of Ps by electrons (Fig. 4) is twice that for hydrogen.

B. Simulation

These cross sections were used to calculate the deposition of positrons in a cylindrical plasma. Physics in the deposition code includes:

- Ionization by and charge exchange with stationary ions
- Ionization by electrons with a Maxwellian velocity distribution (including a finite Ps velocity relative to the average electron velocity)
- Annihilation of Ps in the $J = 0$, $m_J = \pm 1$ state
- Finite spread of the Ps beam in energy and angle
- *o-p* conversion of Ps by impact with electrons and hydrogen atoms.

The plasma was divided into a number of concentric cylindrical shells. The density and temperature are modelled as

$$n_e(r) = n_o\left[1 - \left(\frac{r}{a}\right)^2\right] \tag{6}$$

$$T_e(r) = (T_o - T_a)\left[1 - \left(\frac{r}{a}\right)^2\right]^2 + T_a. \tag{7}$$

The neutral hydrogen density was assumed to decrease exponentially with increasing distance into the plasma[13]

$$n_H(r) = n_H(a)e^{(r-a)/r_H}. \tag{8}$$

The electron density and temperature and neutral hydrogen density for each shell are calculated. The Ps beam is divided into a number of "sub-beams," each of a given energy, angle, and beam strength. The ionization reaction rate for each sub-beam energy is then calculated for each shell. These reaction rates are calculated as

$$\langle \sigma v_{rel} \rangle \equiv \int_0^\infty v^2 dv \int_0^\pi \sin\theta\, d\theta \int_0^{2\pi} d\phi\, v_{rel}\, \sigma(v_{rel})\, f_M(v,\theta,\phi), \tag{9}$$

where the Maxwellian distribution of electrons is given by f_M, $v_{rel} \equiv |\mathbf{v}_{Ps} - \mathbf{v}_e|$, and the reaction rate is a function of the temperature of the shell and the energy

(or velocity) of the Ps sub-beam. Each sub-beam is then followed through the plasma (Fig. 5) and the number of positrons deposited in each shell is determined. Division by the volume of each shell yields the density of positrons deposited in the plasma at the corresponding minor radius.

III. TRANSPORT

A. Processes

The positrons deposited in the plasma are assumed to quickly diffuse along field lines so that the gradient of the positron density has only a radial component. The transport equation can then be expressed as

$$\frac{\partial n}{\partial t} = \frac{1}{r}\frac{\partial}{\partial r} r \left[D(r)\frac{\partial}{\partial r} - V(r) \right] n + S(r,t) - L(r), \tag{10}$$

where the first term in brackets represents the diffusive flux and the second term represents convection. $D(r)$ is the spatially dependent diffusion coefficient and $V(r)$ is the spatially dependent convective velocity. $S(r,t)$ represents sources of positrons, and $L(r)$ represents losses other than transport. The source of positrons is taken as

$$S(r,t) = S(r,0)\delta(t), \tag{11}$$

where $S(r,0)$ is the deposition profile taken from the deposition code and $\delta(t)$ is the Dirac delta function.

B. Losses

Positrons in the plasma may be lost in several different ways before they are transported to the limiter. Positrons can reform positronium in collisions with

neutral hydrogen atoms (Fig. 6).[14] Half of these positronium atoms will be in the shorter lifetime state and will annihilate almost immediately. The rest will either annihilate, pass out of the plasma, or be reionized at a location distant from the positronium formation point. The most likely outcome depends upon the density, temperature, and size of the plasma, as well as the energy of the positronium atom and direction of its travel.

Positrons may also annihilate with plasma electrons. The reaction rate for this process (Fig. 7) is proportional to the electron density and is a function of temperature.[15] At typical tokamak densities and temperatures, however, the lifetime of a positron in a plasma is several orders of magnitude higher than the expected confinement time. At electron densities of 10^{13} cm^{-3}, for example, the lifetime of a positron is about 10 s, while the confinement time might be several tens of milliseconds. Therefore, annihilation with plasma electrons is not expected to be significant.

A third loss mechanism is three-body recombination. That is,

$$e^+ + e^- + e^- \longrightarrow \mathrm{Ps} + e^-. \tag{12}$$

Again, the positronium formed would either annihilate promptly, leave the plasma, or reionize some distance away. The rate of this reaction can be calculated[16] from the electron ionization rate and the principle of detailed balance and can be shown to be insignificant (lifetime of $\sim 10^{35}$ s for typical parameters) at energies near or greater than the ionization potential of positronium.

C. Simulation

A diffusion code has been written to solve for $n(r,t)$ given initial conditions from the deposition code. It is a finite difference code which requires the positron density to be zero at $r = a$ and its derivative to be zero at $r = 0$. At each iteration of the finite difference scheme, the change in the positron density due to diffusion, convection, annihilation, and Ps formation is calculated. The number of positrons in the outermost shell is then divided by the time interval between iterations. The annihilation signal is given by this value. The number of positrons in this shell is then set to zero to simulate loss of positrons to the limiter.

IV. ANALYSIS AND EXAMPLES

For the examples here, the parameters of the Texas Experimental Tokamak[17] (TEXT) will be used. TEXT has a major radius of 100 cm and a minor radius of 28 cm. Electron densities in the range 10^{13}–10^{14} cm^{-3} and central temperatures of 1 keV are common. The confinement time is in the range of 20–40 ms. These parameters are nearly ideal for a positron transport experiment.

A. Deposition

The positronium beam distribution is taken to be that produced by passing a 1 keV beam of positrons through a 50-Å carbon film[2]:

$$dN = (10^{-3}\ \text{eV})^{\frac{1}{2}} E^{-\frac{3}{2}}\, dE\, d\Omega, \tag{13}$$

where dN is the positronium distribution per positron incident on the film. The carbon film is located 100 cm from the magnetic axis of the plasma and the beam is apertured so that it extends $\pm 5°$ vertically and horizontally about the beam axis. Figure 8 shows a typical deposition profile. The beam axis may be moved or the collimation changed to allow positrons to be deposited centrally or radially displaced making measurements sensitive to the transport at various locations in the plasma possible.

Deposition simulations at increasing electron density ranging from 10^{12} to 10^{16} cm^{-3} (Fig. 9) show two density regimes. At densities below a critical electron density, $\overline{n_{ec}}$, determined by the size of the plasma and the energy distribution of the positronium, the number of positrons, N_{e+}, is proportional to the electron density. Above $\overline{n_{ec}}$, N_{e+} asymptotically approaches 100% of the positrons which arrive at the near edge of the plasma before annihilating. For the parameters used in this simulation, $\overline{n_{ec}} \simeq 10^{14}$ cm^{-3}. Below $\overline{n_{ec}}$, the deposition profiles have the same shape, but differ in magnitude. In this regime, the plasma is transparent to positronium. Above $\overline{n_{ec}}$, the profiles become more outwardly peaked as the positronium beam becomes less able to penetrate the plasma. Here, the plasma is opaque. A good positron transport experiment requires large numbers of positrons deposited near the center of the plasma, so the ideal density is equal to or slightly less than the critical density which, fortunately and coincidentally, is the normal operating range of most tokamaks.

The deposition of positrons can be thought of as a balance between two processes. The positronium must be energetic enough to pass through the plasma before it annihilates, but not so energetic that it passes through the plasma

without being ionized. Since the ionization cross section drops quickly at large energy, there is a peak positronium energy at which the probability of ionization is maximized. This energy depends upon the electron density and temperature of the plasma and the distance from the carbon film (or other Ps-forming device) to the plasma. Figure 10 shows the dependence of the ionization probability on the Ps energy at different electron densities. Below $\overline{n_{ec}}$, the ionization fraction is proportional to $\overline{n_e}$, but approaches a limit above $\overline{n_{ec}}$. At higher energies, the curves do not approach the limit as quickly, demonstrating the energy dependence of $\overline{n_{ec}}$. From this, it can be deduced that positronium atoms with energy in the range of 200–300 eV have the best probability of being ionized for plasma parameters of interest with rates approaching 30% possible at densities of 10^{14} cm^{-3}.

B. Transport

The three dominant processes affecting the transport of positrons in a tokamak plasma are diffusion, convection, and positronium formation. In the simulations here, the convection was modelled by assuming a convective velocity

$$V(r) = V_o \left(\frac{r}{a}\right), \tag{14}$$

where V_o was typically in the range -1000 to -2000 cm s^{-1}. (The minus sign indicates that the convection is radially inward.) The diffusion coefficient was taken to be in the range 5000 to 20,000 cm^2 s^{-1}, and could be spatially varying. The neutral hydrogen density, which affects the positronium formation rate, was assumed to decrease exponentially from the edge of the plasma inward. The neutral edge density was taken as 3×10^{10} cm^{-3}, with the density falling

by a factor of two every 3 cm.[13] The neutral hydrogen density is not isotropic in toroidal angle, but is instead peaked at the limiter. For these simulations, a toroidally averaged density was used. Figure 6b shows that the reaction rate for the formation of positronium is peaked for temperatures found near the edge of the plasma. Combining this with the fact that the neutral hydrogen density is highest at the edge demonstrates that positronium formation is most likely near the edge of the plasma. If the temperature at the edge of the plasma is 10 eV and the neutral hydrogen density is 2×10^{10} cm^{-3}, an average positron will last approximately 1 ms in this region before being reconverted into a positronium atom. This edge region is thin, however, as the reaction rate is a strong function of temperature and the neutral hydrogen density falls off quickly from the edge of the plasma inwards. Significant conversion can still take place since all the positrons must pass through this region before striking the limiter. In order to prevent a majority of the positrons from forming positronium, the neutral hydrogen density must be kept lower than a few times 10^{10} cm^{-3} at the edge for the plasma conditions assumed in these simulations.

In each of the transport simulations, the annihilation signal shows two distinct regions. After a time on the order of the confinement time, the signal decays exponentially with a fixed time constant representing the decay time of the lowest order solution of the transport equation (Eq. 10). Before the signal reaches this state, it demonstrates different types of behavior, including decaying exponentially with shorter time constants. In this region, the higher order modes are contributing to the signal.

By injecting positrons into the center of the plasma, a deposition profile

which is very similar in shape to the lowest order eigenfunction of the transport equation is obtained. Because of this, the other modes quickly relax so that they do not contribute as much to the signal. However, by injecting at an angle to the center, a deposition profile peaked nearer the edge of the plasma can result. In the decay of this profile, the higher order modes are more dominant than for central deposition. Analysis of the signal then shows two or more time constants in the decay. By identifying and analyzing these time constants, quantitative information about the spatial dependence of the diffusion coefficients can be obtained.

Figures 11 and 12 show simulations of the annihilation signals from two different profiles, one center and one edge deposition. Least-squares fits (Table 1) to these simulations make it possible to identify the two lowest-order decay constants (Tables 2 and 3). Adding random errors to simulate the statistics of averaging over 100 shots still allows fits to be made fairly accurately. For Fig. 11, D was constant. For Fig. 12, D inside $r = a/2$ was twice what is was outside $r = a/2$.

C. Analysis

Measuring τ_1 and τ_2 allows the differentiation of constant and varying D profiles. This can be accomplished by solving the transport equation (Eq. 10) given a model for the diffusion coefficient and the convective velocity. The effects of the neutral hydrogen can be taken into account by realizing that in some thin layer near the edge, positronium formation may be the dominant loss process. This loss will reduce the positron density near the edge, reducing the effective

minor radius of the plasma as if the neutral hydrogen were an extension of the limiter. Thus, positronium formation manifests itself as an effective reduction in the minor radius of the plasma and an accompanying reduction in the time constants of the decay, as well as a reduction in the amplitude of the signal.

Table 4 shows the results of using a finite-difference predictor-corrector code to solve for the time constants of the solutions to the transport equation using the same model for the diffusion coefficient as was used to generate the annihilation signals and assuming the convective velocity to be known (as from a Ware pinch calculation or similar model). For these determinations, the effective reduction of the minor radius due to positronium formation was taken as 2 cm. Different values of D_1 and D_2 were used until a solution was found in which τ_1 was equal to the average of the τ_1's generated by the center and edge deposition runs, and τ_2 was equal to the τ_2 generated from the edge deposition run. The results show that it is possible to differentiate between constant and varying diffusion coefficients.

V. CONCLUSION

These results show that a positron transport experiment is feasible using technology currently being developed. The densities and temperatures of today's tokamaks are ideally suited for positron deposition by ionization of hundred eV-range positronium beams. Positronium formation by impact of positrons on neutral hydrogen atoms is a major source of loss of positrons from the plasma, so the density of neutral hydrogen must be kept low in order to avoid losing too much signal. By measuring the different time constants of the

decay, the diffusion and convection of positronium can be studied with spatial resolution. The results of such an experiment will provide a new means for studying the transport of electron-mass particles in tokamaks.

ACKNOWLEDGMENTS

The author thanks R. J. Drachman and S. F. Cordes for discussions on the physics of positronium and R. Olson for providing the ionization and charge-exchange cross sections for Ps-p collisions. The author also thanks C. M. Surko and J. D. Strachan for advice on how to proceed with this work. W. L. Rowan provided the transport models used in this analysis. This work was supported by the United States Department of Energy under contract DE–AC02–76–CHO–3073.

References

[1]C. M. Surko, M. Leventhal, W. S. Crane, A. P. Mills, Jr., H. Kugel, and J. Strachan, *Positrons and Solids, Surfaces, and Atoms*, edited by K. F. Canter, W. S. Crane, and A. P. Mills, Jr. (World Scientific, Singapore, 1986); C. M. Surko, M. Leventhal, W. Crane, A. P. Mills, Jr., H. Kugel, J. Strachan, and T. J. Murphy, *Bull. Am. Phys. Soc.* **30**, 1416 (1985); C. M. Surko, M. Leventhal, W. S. Crane, A. Passner, F. Wysocki, T. J. Murphy, J. Strachan, and W. L. Rowan, *Rev. Sci. Instrum.* **57**, 1862 (1986).

[2]A. P. Mills, Jr. and William S. Crane, *Phys. Rev.* **A31**, 593 (1985).

[3]Stephan Berko and Hugh N. Pendleton, *Ann. Rev. Nucl. Part. Sci.* **30**, 543 (1980).

[4]Arthur Rich, *Rev. Mod. Phys.* **53**, 127 (1981).

[5]Otto Halpern, *Phys. Rev.* **94**, 904 (1954).

[6]S. J. Ward, J. W. Humberston, and M. R. C. McDowell, *J. Phys. B* **18**, L525 (1985).

[7]S. Hara and P. A. Fraser, *J. Phys. B* **8**, L472 (1975).

[8]A. S. Baltenko and I. D. Segal, *Sov. Phys. Tech. Phys.* **28**, 508 (1983).

[9]Richard J. Drachman, private communication.

[10]R. Olson, private communication.

[11]R. E. Olson and A. Salop, *Phys. Rev.* **A14**, 579 (1976).

[12]M. Gryziński, *Atomic Collision Processes*, edited by M. R. C. McDowell (North-Holland Publishing Co., Amsterdam, 1964), pp. 226–236.

[13]W. L. Rowan, private communication.

[14]E. Ficocelli Varracchio and M. D. Girardeau, *J. Phys. B* **16**, 1097 (1983).

[15]A. S. Baltenkov and V. B. Gilerson, *Sov. J. Plasma Phys.* **10**, 632 (1984).

[16]Kenneth R. Lang, *Astrophysical Formulae* (Springer-Verlag, Berlin, 1980), p. 102.

[17]K. W. Gentle, *Nucl. Tech./Fusion* **1**, 479 (1981).

Tables

TABLE I. Fits to a two-time-constant exponential decay with and without statistical errors added, demonstrating the usefulness of the fitting routine. The errors added were similar to those expected from averaging one hundred runs.

Run	A_1	τ_1	A_2	τ_2
Generated	15.00	20.00	40.00	2.50
w/error	15.06	19.75	40.69	2.51

TABLE II. Fits to the annihilation signal using a one- or two-time-constant exponential decay for the signal with and without statistical errors added. For these runs, $D = 10000$ cm^2 s^{-1} and $V_o = -1000$ cm s^{-1}.

Run	A_1	τ_1	A_2	τ_2
Center	32.95	20.08		
w/error	32.73	20.13		
Edge	13.45	19.84	41.70	2.42
w/error	13.29	19.87	43.48	2.39

TABLE III. Fits to the annihilation signal using a one- or two-time-constant exponential decay for the signal with and without statistical errors added. For these runs $D = 15000$ cm^2 s^{-1} inside $r = a/2$, and 7500 outside $r = a/2$, and $V_o = -1000$ cm s^{-1}.

Run	A_1	τ_1	A_2	τ_2
Center	20.64	26.21		
w/error	20.54	26.23		
Edge	8.88	26.14	31.32	2.31
w/error	9.19	25.25	38.73	2.04

TABLE IV. Diffusion coefficients used in the transport simulations and those derived from the time constants of the positron signal decay.

Run	Actual		Calculated	
	D_1	D_2	D_1	D_2
1	10000	10000	10230	9580
2	15000	7500	20000	7580

Figures

FIG. 1. Cross section for *o-p* conversion of positronium by impact of electrons, calculated from partial-wave phase shifts presented in Ref. 6.

FIG. 2. Cross section for *o-p* conversion of positronium by impact of Ps on hydrogen atoms, interpolated from cross sections presented in Ref. 7.

FIG. 3. Cross sections for the ionization and charge exchange of positronium with protons interpolated from cross sections provided by R. Olson in Ref. 10.

FIG. 4. Cross section for the ionization of positronium by electrons calculated classically by modifying the Gryziński expression for the ionization of hydrogen by electrons.

FIG. 5. Diagram showing the scheme used to divide the plasma into shells of constant density, temperature, etc., and the model of the positronium beam used.

FIG. 6. Cross section (a) and the reaction rate (b) for the formation of positronium by impact of positrons on neutral hydrogen atoms as presented in Ref. 14. The three cross sections represent three different models used in calculating the cross section in that reference.

FIG. 7. Lifetime of positrons in a plasma presented as the product $n_e\tau$, as presented in Ref. 15.

FIG. 8. Typical deposition profiles for positrons in a TEXT-sized device. $\overline{n_e} = 3 \times 10^{13}$ cm^{-3}, $T_o = 1$ keV, number of positrons incident on the carbon film $= 5 \times 10^9$, and the total number of positrons deposited in the plasma

is 1.3×10^5. Figure (a) represents central deposition and (b) represents deposition from a beam aimed 10° up or down from center.

FIG. 9. Number of positrons deposited in the plasma *vs.* $\overline{n_e}$. The number of positrons incident on the carbon film was 5×10^9. The dotted line represents the number of positrons reaching the near edge of the plasma and is a limit reached when the plasma becomes "opaque" to positrons. The critical electron density, $\overline{n_{ec}}$, can be seen from this plot to lie near 10^{14} cm^{-3}.

FIG. 10. Fraction of positronium atoms ionized as a function of positronium energy, with electron density as a parameter. The dotted line represents the fraction of positronium atoms reaching the plasma before annihilating and is an absolute limit on the ionization fraction.

FIG. 11. Simulated positron annihilation signals from (o) center and (•) edge deposition of positrons with fits to one- or two-time-constant exponential decays for a constant D model.

FIG. 12. Simulated positron annihilation signals from (o) center and (•) edge deposition of positrons with fits to one- or two-time-constant exponential decays for a model in which D is larger inside than it is outside $r = a/2$.

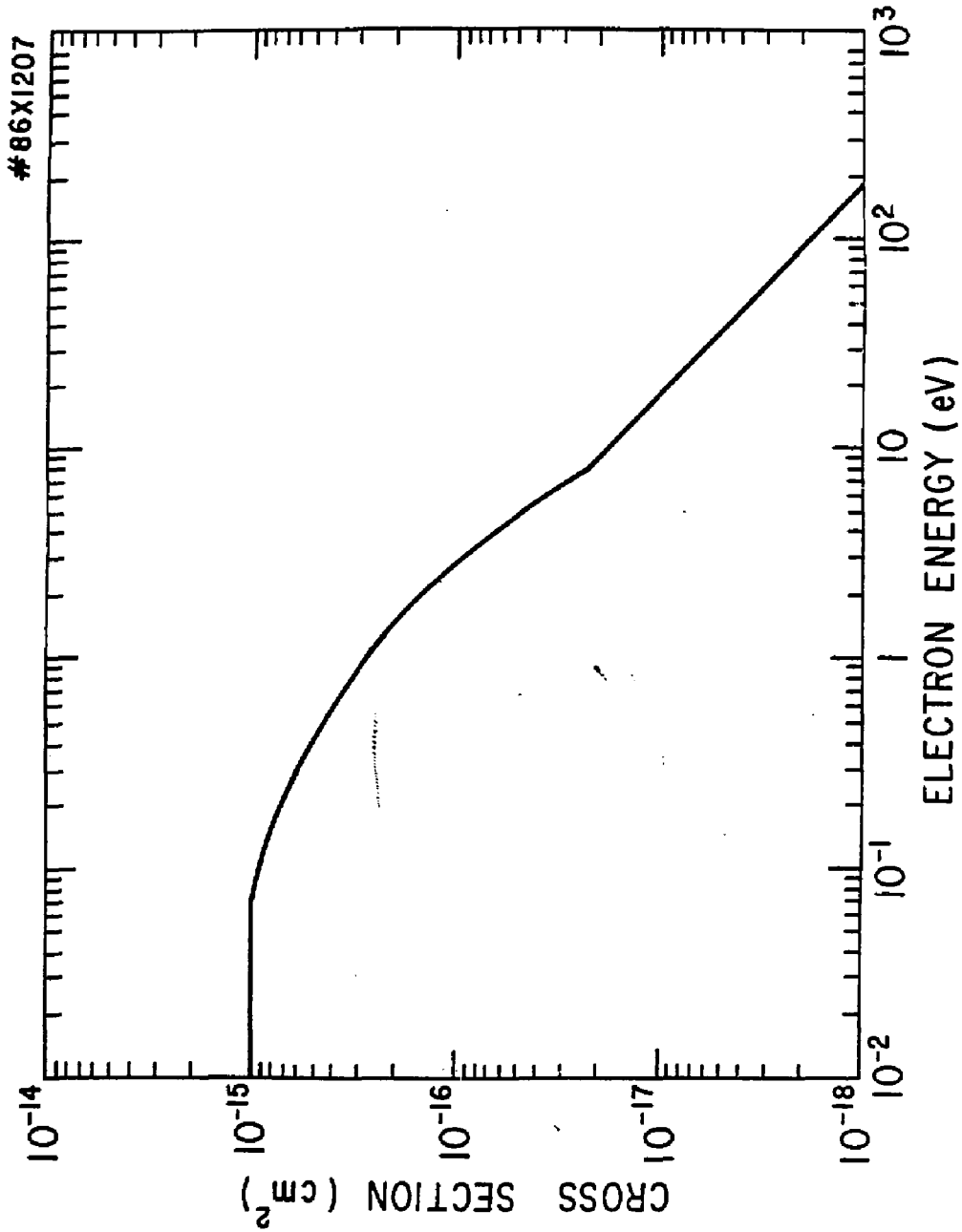
#86X1207
CROSS SECTION (cm²)
ELECTRON ENERGY (eV)
10⁻¹⁴
10⁻¹⁵
10⁻¹⁶
10⁻¹⁷
10⁻¹⁸
10⁻²
10⁻¹
1
10
10²
10³

Fig. 1

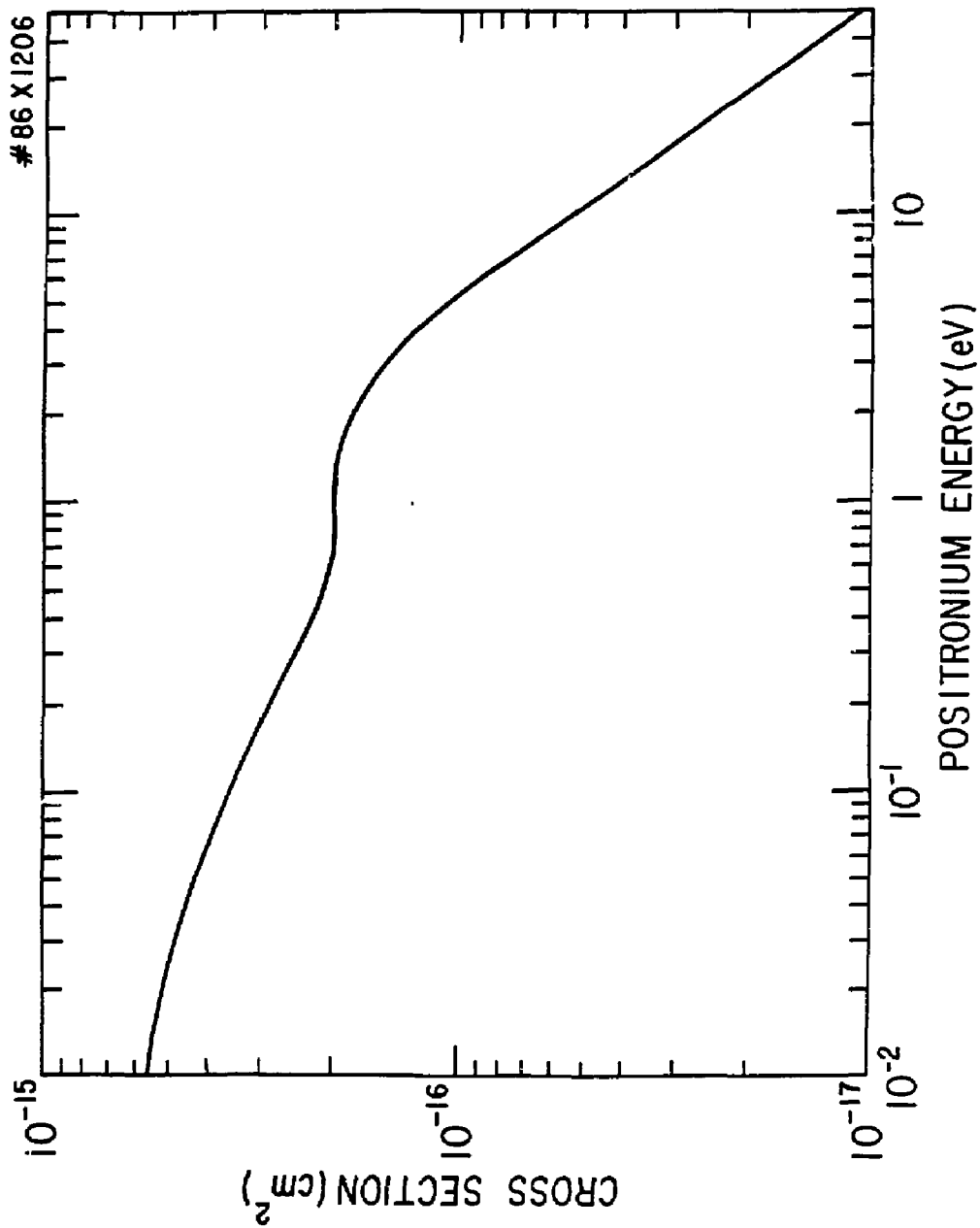
#86 X1206
CROSS SECTION (cm^2)
10^{-15}
10^{-16}
10^{-17}
10^{-2}
10^{-1}
1
10
POSITRONIUM ENERGY (eV)

Fig. 2

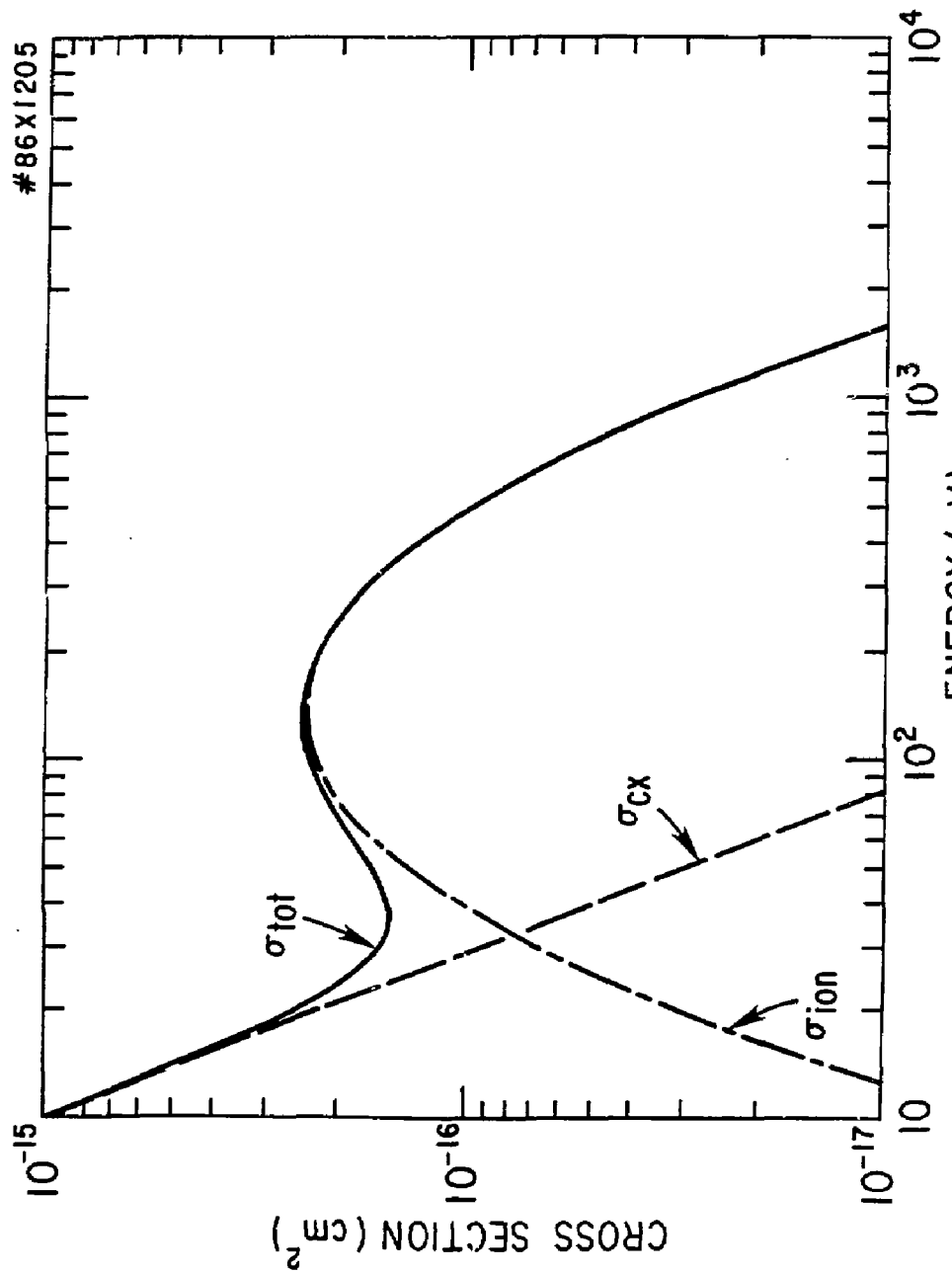
#86X1205
CROSS SECTION (cm²)
ENERGY (eV)
σtot
σcx
σion
10⁻¹⁵
10⁻¹⁶
10⁻¹⁷
10
10²
10³
10⁴

Fig. 3

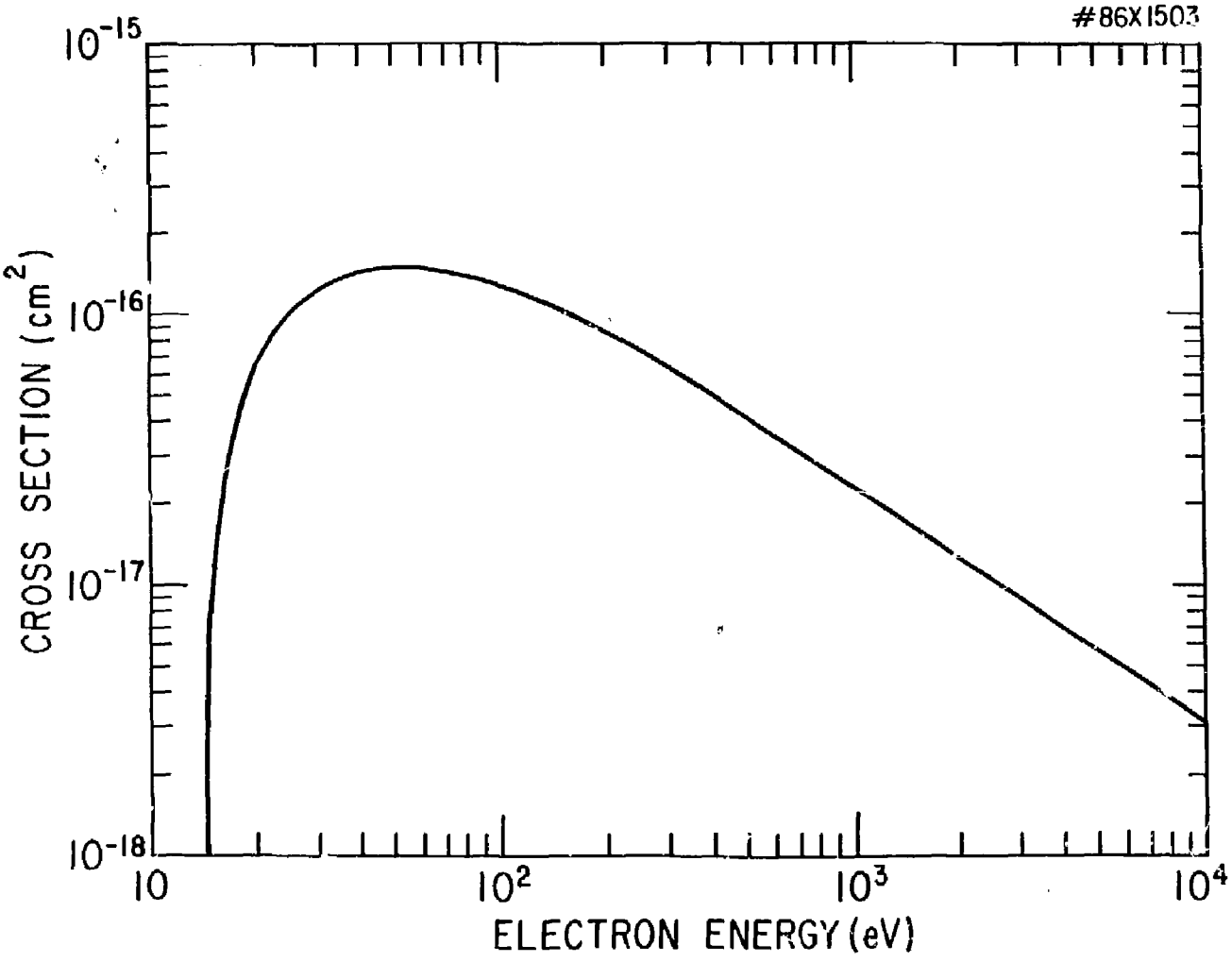
#86X1503
10^{-15}
10^{-16}
10^{-17}
10^{-18}
CROSS SECTION (cm^2)
10
10^2
10^3
10^4
ELECTRON ENERGY (eV)

Fig. 4

#86X1204

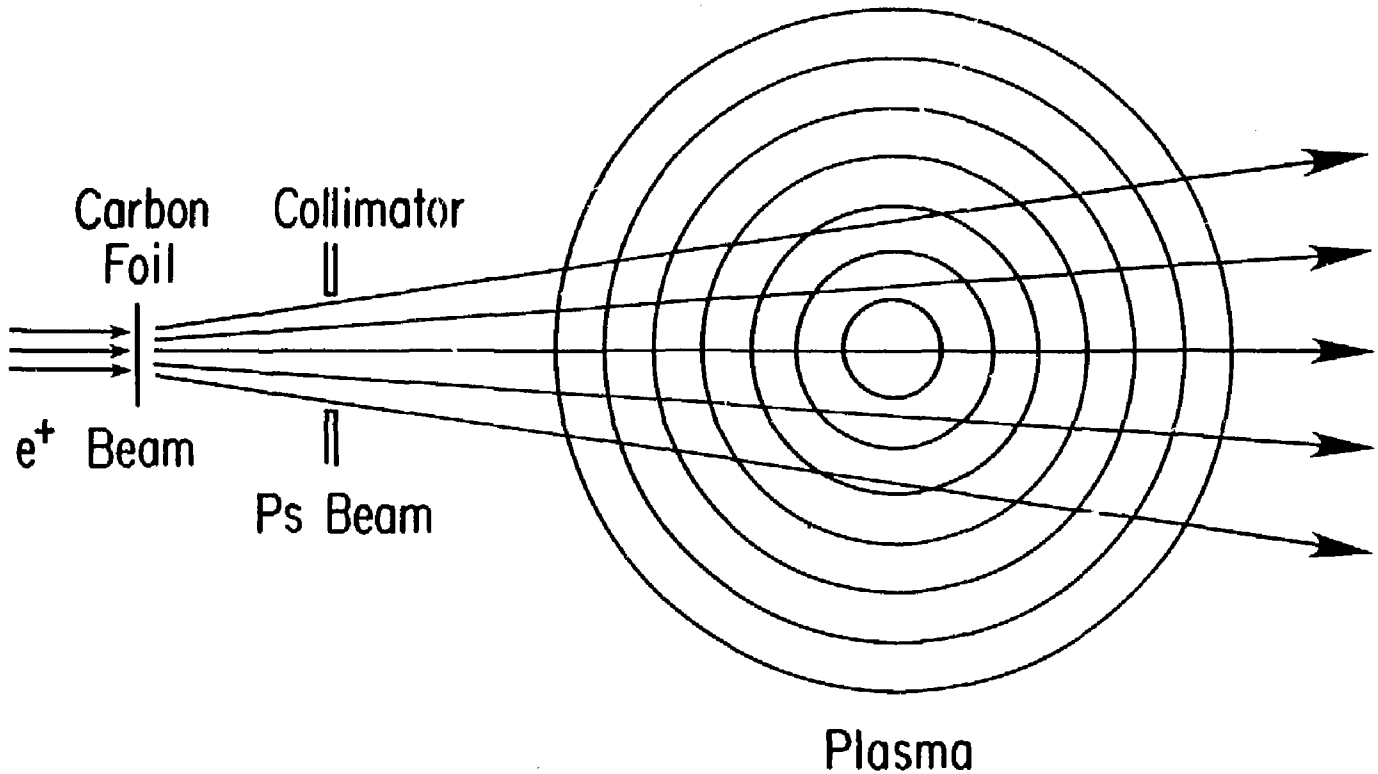

Fig. 5

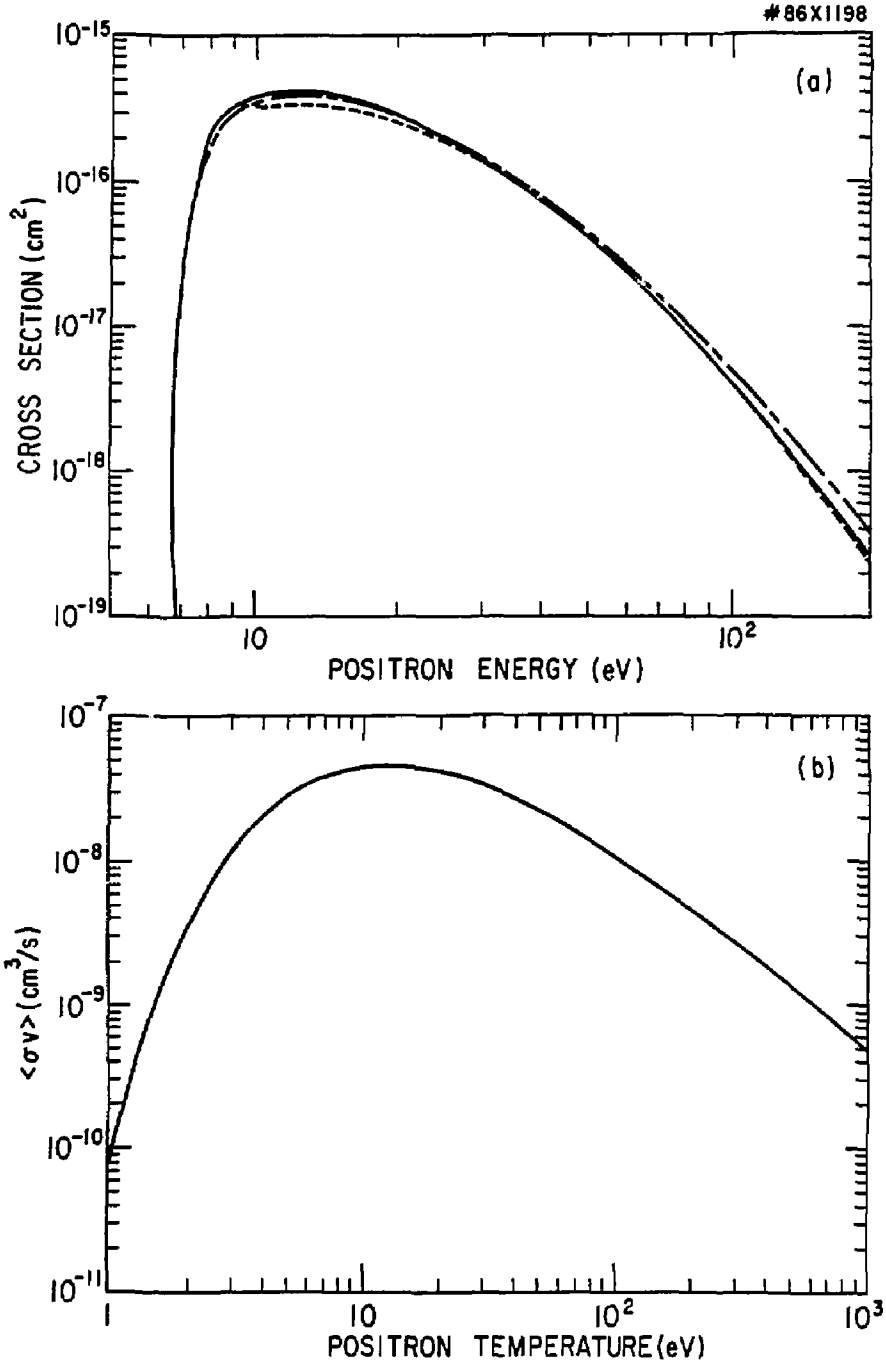
#86X1198
(a)
CROSS SECTION (cm²)
10⁻¹⁵
10⁻¹⁶
10⁻¹⁷
10⁻¹⁸
10⁻¹⁹
10
10²
POSITRON ENERGY (eV)
(b)
<σv> (cm³/s)
10⁻⁷
10⁻⁸
10⁻⁹
10⁻¹⁰
10⁻¹¹
1
10
10²
10³
POSITRON TEMPERATURE (eV)

Fig. 6

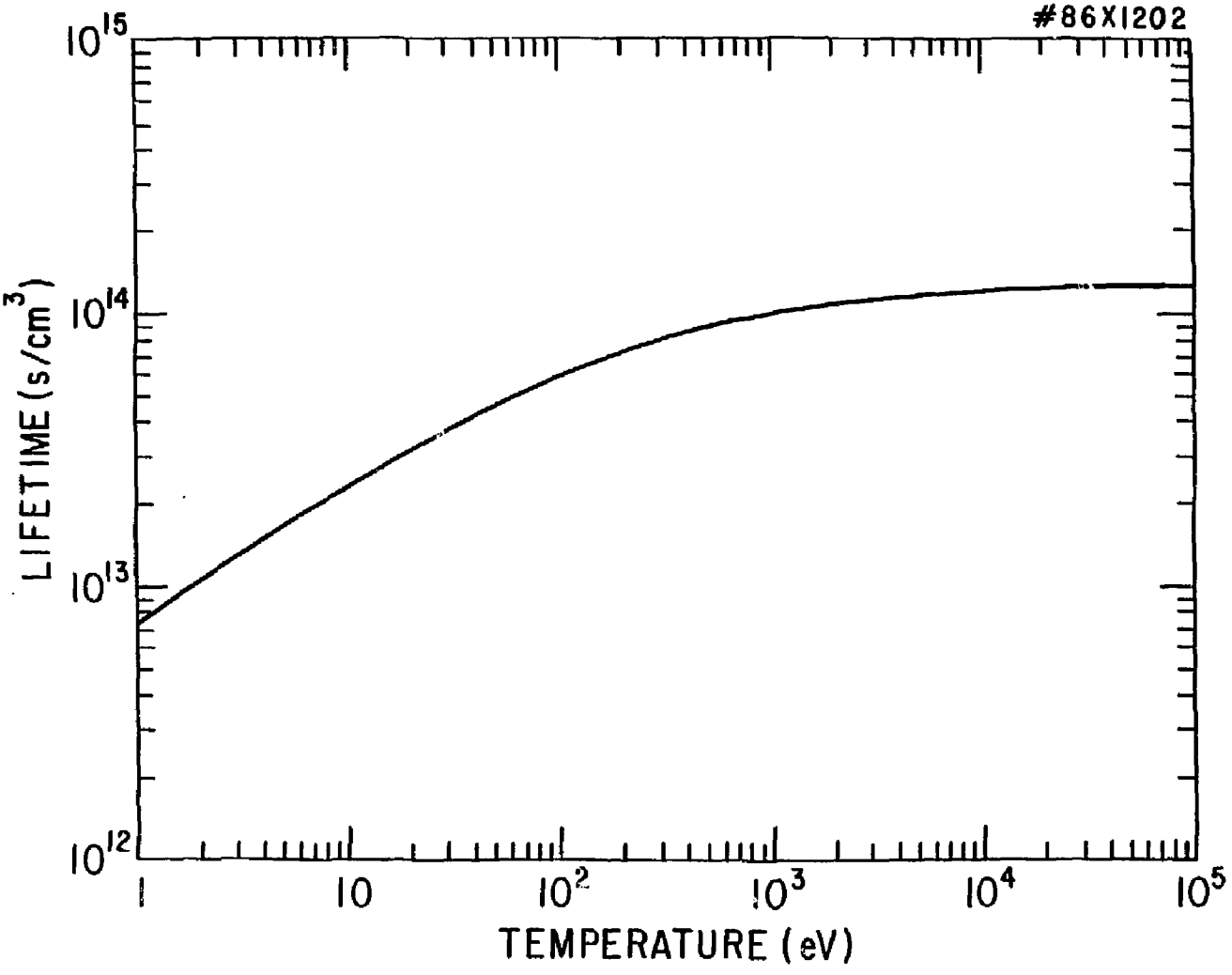
#86X1202
10^{15}
10^{14}
10^{13}
10^{12}
LIFETIME (s/cm^3)
1
10
10^2
10^3
10^4
10^5
TEMPERATURE (eV)

Fig. 7

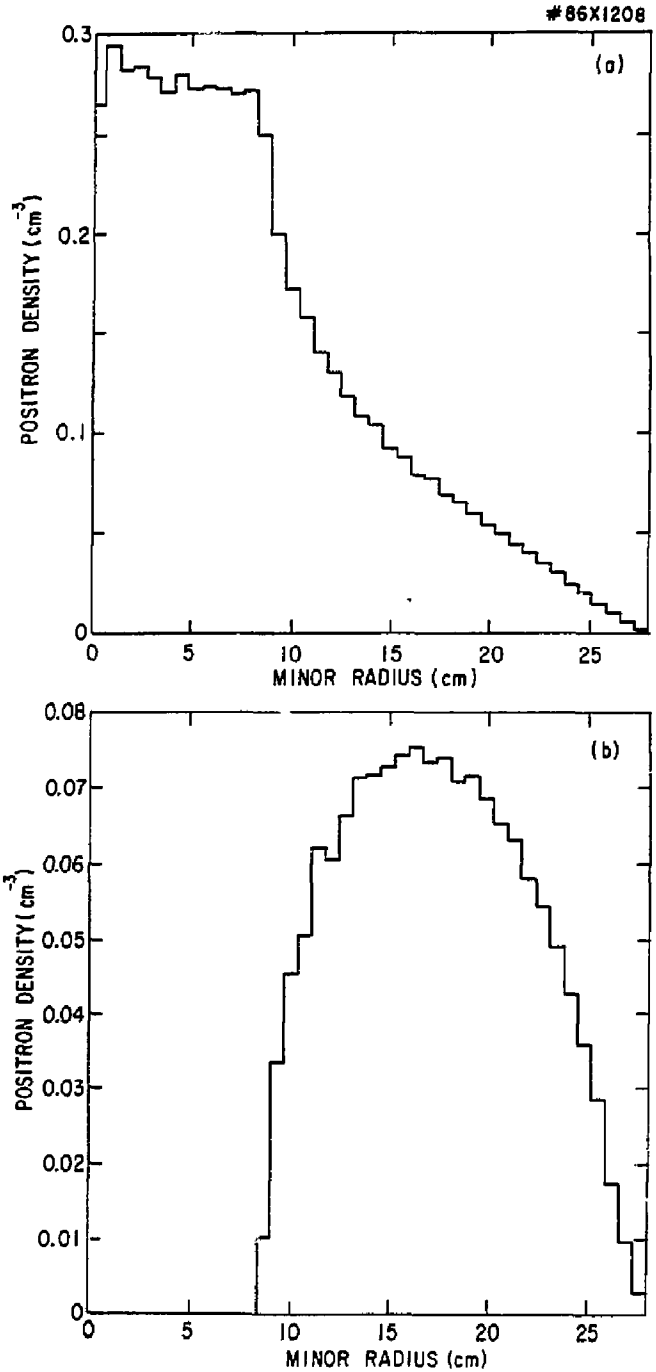
#86X1208
(a)
POSITRON DENSITY (cm^{-3})
0.3
0.2
0.1
0
0
5
10
15
20
25
MINOR RADIUS (cm)
(b)
POSITRON DENSITY (cm^{-3})
0.08
0.07
0.06
0.05
0.04
0.03
0.02
0.01
0
0
5
10
15
20
25
MINOR RADIUS (cm)

Fig. 8

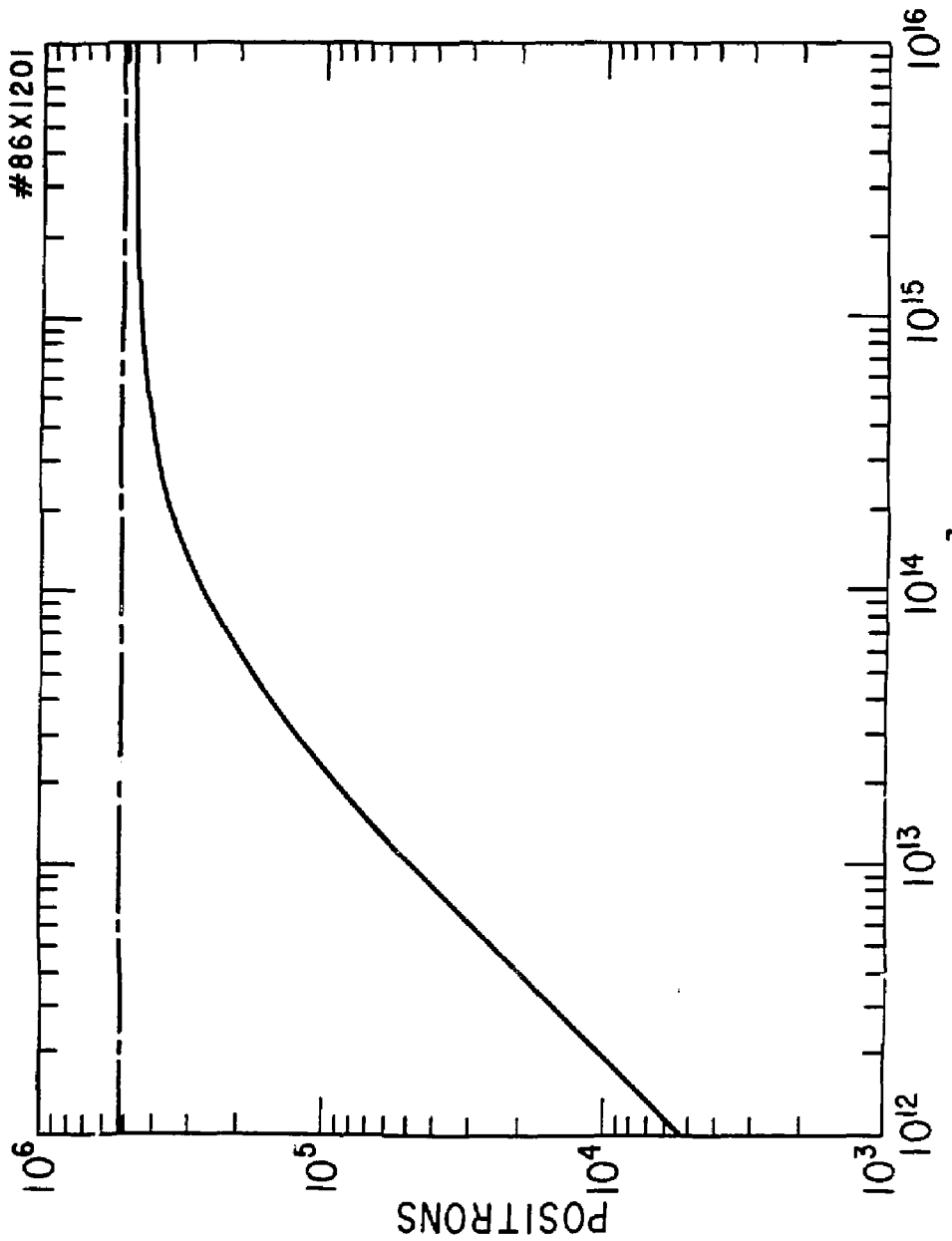
#86X1201
POSITRONS
10^6
10^5
10^4
10^3
10^{12}
10^{13}
10^{14}
10^{15}
10^{16}
$\bar{n}_e$ (cm^{-3})

Fig. 9

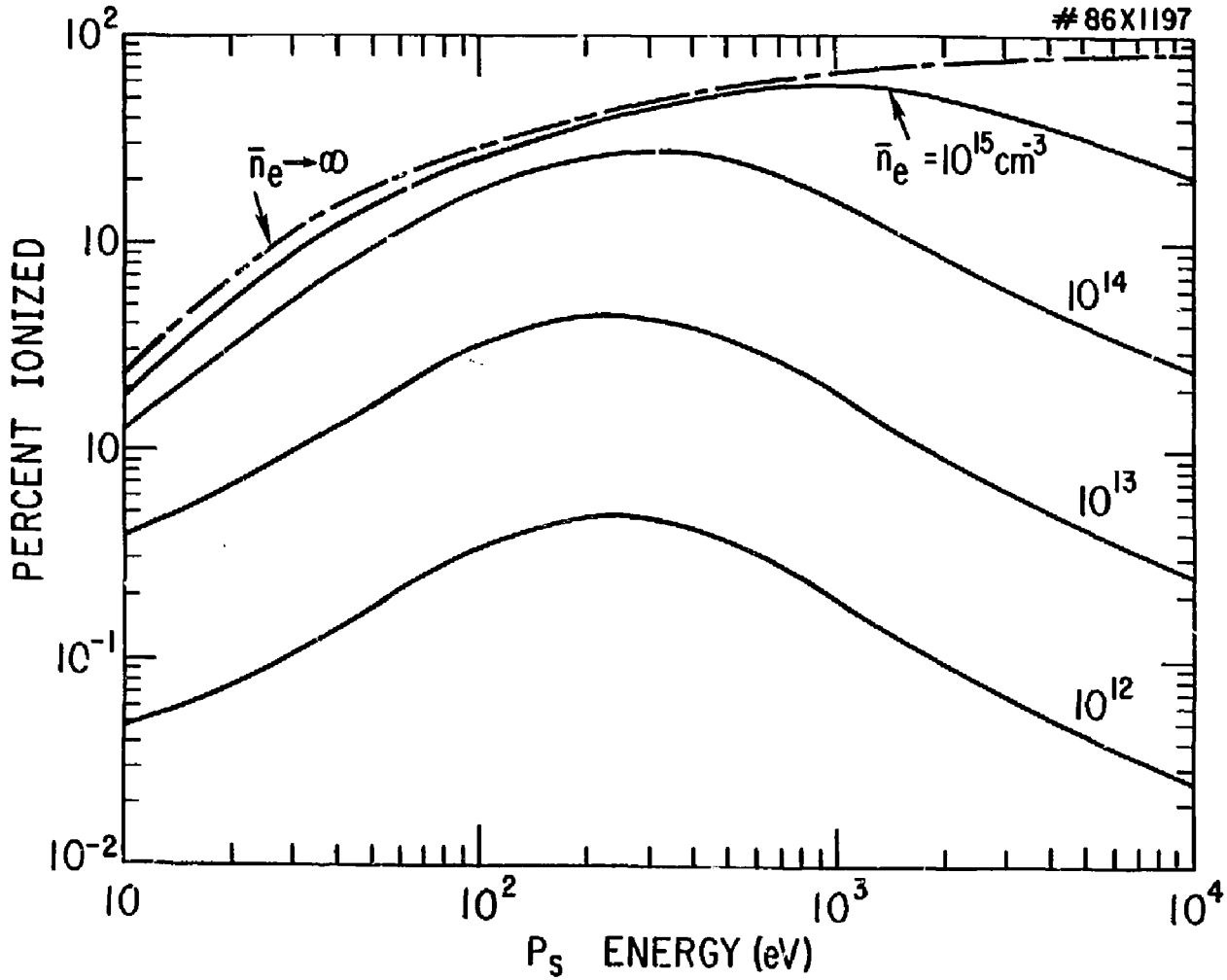
#86X1197
PERCENT IONIZED
10^2
10
1
10^{-1}
10^{-2}
$\bar{n}_e \to \infty$
$\bar{n}_e = 10^{15} cm^{-3}$
10^{14}
10^{13}
10^{12}
10
10^2
10^3
10^4
P_S ENERGY (eV)

Fig. 10

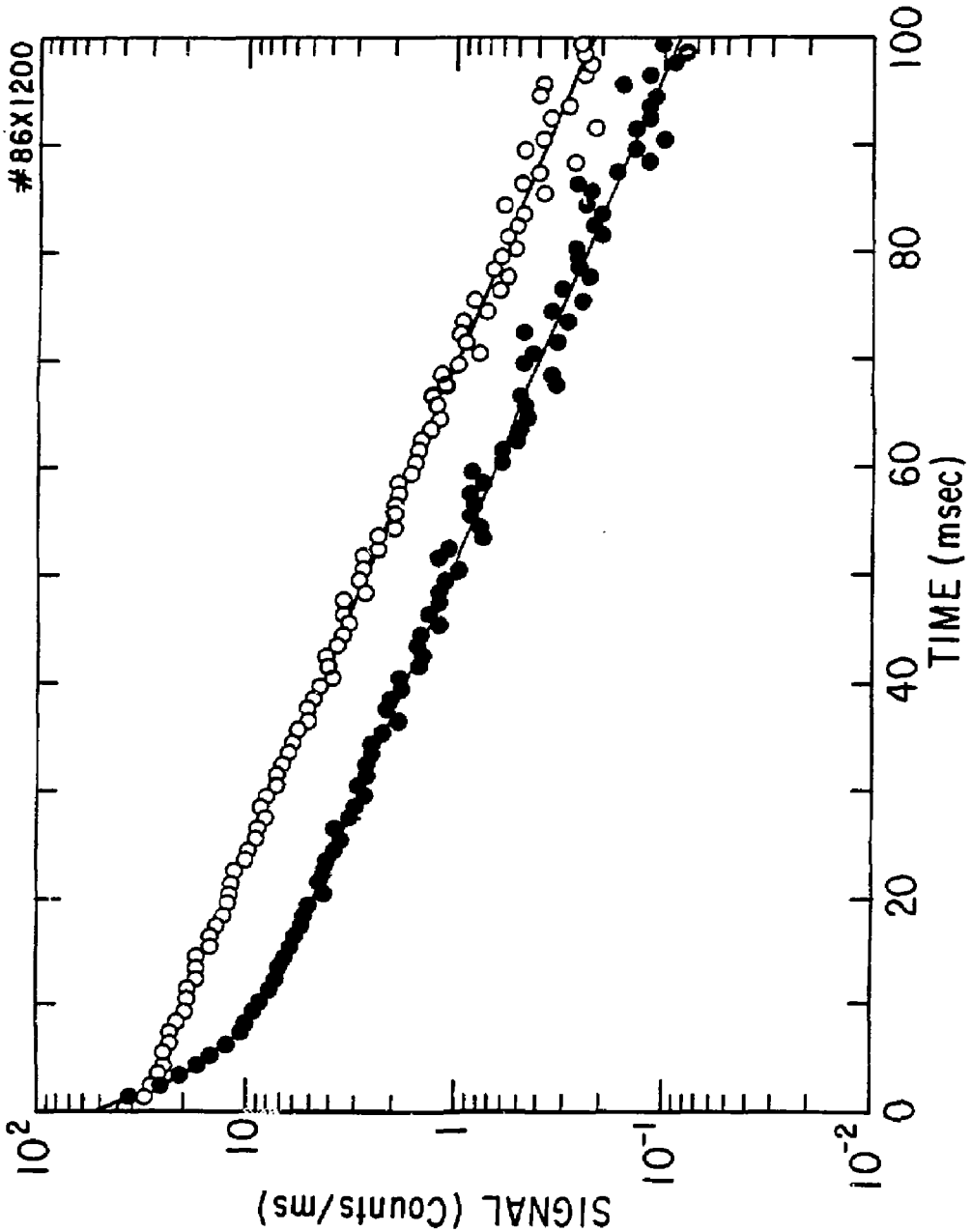
#86X1200
SIGNAL (Counts/ms)
10^2
10
1
10^{-1}
10^{-2}
0
20
40
60
80
100
TIME (msec)

Fig. 11

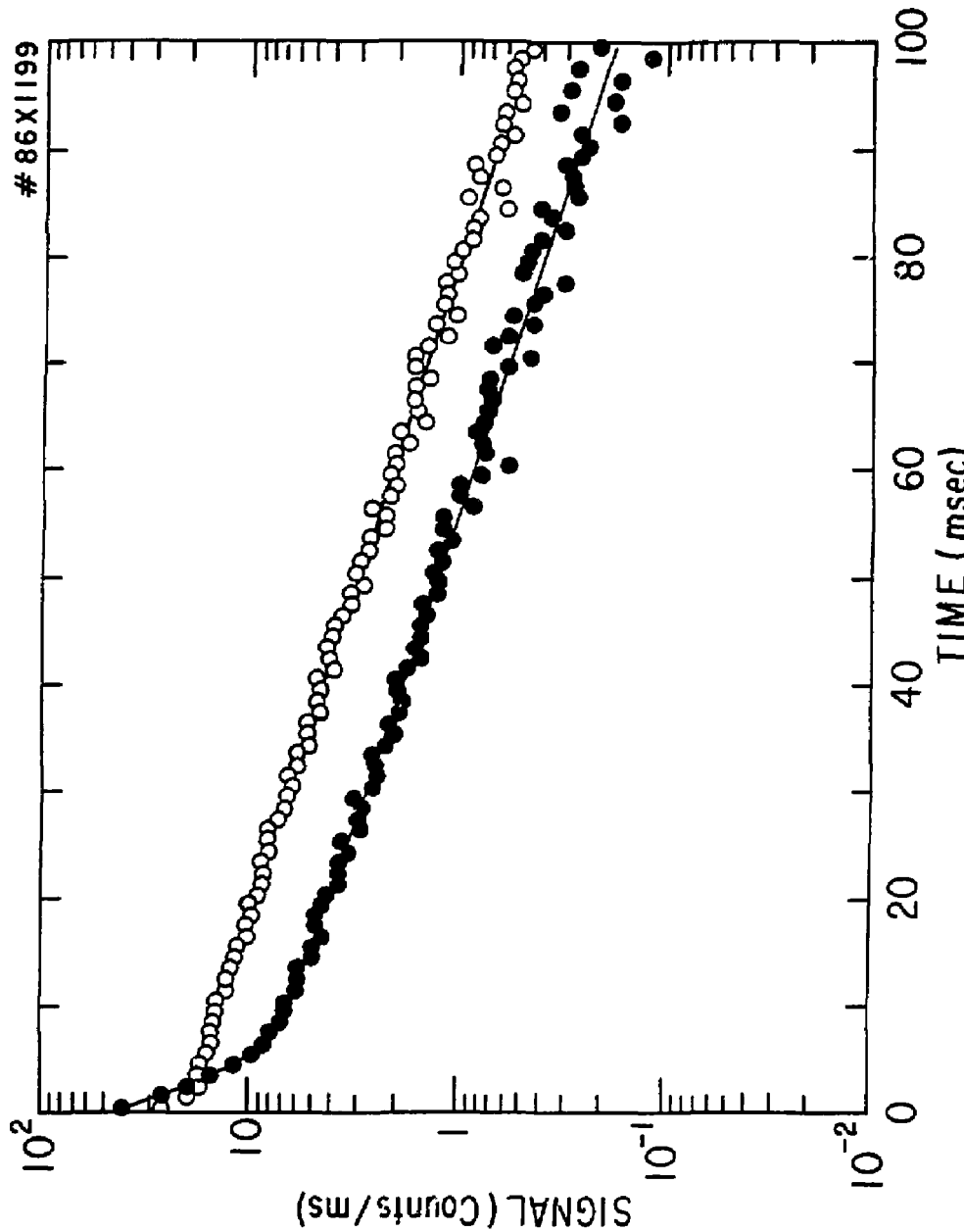
#86X1199
SIGNAL (Counts/ms)
TIME (msec)
10^2
10
1
10^{-1}
10^{-2}
0
20
40
60
80
100

Fig. 12

EXTERNAL DISTRIBUTION IN ADDITION TO UC-20

Plasma Res Lab, Austra Nat'l Univ, AUSTRALIA
Dr. Frank J. Paoloni, Univ of Wollongong, AUSTRALIA
Prof. I.R. Jones, Flinders Univ., AUSTRALIA
Prof. M.H. Brennan, Univ Sydney, AUSTRALIA
Prof. F. Cap, Inst Theo Phys, AUSTRIA
M. Goossens, Astronomisch Instituut, BELGIUM
Prof. R. Boucique, Laboratorium voor Natuurkunde, BELGIUM
Dr. D. Palumbo, Dg XII Fusion Prog, BELGIUM
Ecole Royale Militaire, Lab de Phys Plasmas, BELGIUM
Dr. P.H. Sakanaka, Univ Estadual, BRAZIL
Lib. & Doc. Div., Instituto de Pesquisas Espaciais, BRAZIL
Dr. C.R. James, Univ of Alberta, CANADA
Prof. J. Teichmann, Univ of Montreal, CANADA
Dr. H.M. Skarsgard, Univ of Saskatchewan, CANADA
Prof. S.R. Sreenivasan, University of Calgary, CANADA
Prof. Tudor W. Johnston, INRS-Energie, CANADA
Dr. Hannes Barnard, Univ British Columbia, CANADA
Dr. M.P. Bachynski, MPB Technologies, Inc., CANADA
Chalk River, Nucl Lab, CANADA
Zhengwu Li, SW Inst Physics, CHINA
Library, Tsing Hua University, CHINA
Librarian, Institute of Physics, CHINA
Inst Plasma Phys, Academia Sinica, CHINA
Dr. Peter Lukac, Komenskeho Univ, CZECHOSLOVAKIA
The Librarian, Culham Laboratory, ENGLAND
Prof. Schatzman, Observatoire de Nice, FRANCE
J. Radet, CEN-BP6, FRANCE
JET Reading Room, JET Joint Undertaking, ENGLAND
AM Dupas Library, AM Dupas Library, FRANCE
Dr. Tom Mual, Academy Bibliographic, HONG KONG
Preprint Library, Cent Res Inst Phys, HUNGARY
Dr. R.K. Chhajlani, Vikram Univ, INDIA
Dr. B. Dasgupta, Saha Inst, INDIA
Dr. P. Kaw, Physical Research Lab, INDIA
Dr. Phillip Rosenau, Israel Inst Tech, ISRAEL
Prof. S. Cuperman, Tel Aviv University, ISRAEL
Prof. G. Rostagni, Univ Di Padova, ITALY
Librarian, Int'l Ctr Theo Phys, ITALY
Miss Clelia De Palo, Assoc EURATOM-ENEA, ITALY
Biblioteca, del CNR EURATOM, ITALY
Dr. H. Yamato, Toshiba Res & Dev, JAPAN
Direc. Dept. Lg. Tokamak Dev. JAERI, JAPAN
Prof. Nobuyuki Inoue, University of Tokyo, JAPAN
Research Info Center, Nagoya University, JAPAN
Prof. Kyoji Nishikawa, Univ of Hiroshima, JAPAN
Prof. Sigeru Mori, JAERI, JAPAN
Prof. S. Tanaka, Kyoto University, JAPAN
Library, Kyoto University, JAPAN
Prof. Ichiro Kawakami, Nihon Univ, JAPAN
Prof. Satoshi Itoh, Kyushu University, JAPAN
Dr. D.I. Choi, Adv. Inst Sci & Tech, KOREA
Tech Info Division, KAERI, KOREA
Bibliotheek, Fom-Inst Voor Plasma, NETHERLANDS
Prof. B.S. Liley, University of Waikato, NEW ZEALAND
Prof. J.A.C. Cabral, Inst Superior Tecn, PORTUGAL
Dr. Octavian Petrus, ALI CUZA University, ROMANIA
Prof. M.A. Hellberg, University of Natal, SO AFRICA
Dr. Johan de Villiers, Plasma Physics, Nucor, SO AFRICA
Fusion Div. Library, JEN, SPAIN
Prof. Hans Wilhelmson, Chalmers Univ Tech, SWEDEN
Dr. Lennart Stenflo, University of UMEA, SWEDEN
Library, Royal Inst Tech, SWEDEN
Centre de Recherchesen, Ecole Polytech Fed, SWITZERLAND
Dr. V.T. Tolok, Kharkov Phys Tech Ins, USSR
Dr. D.D. Ryutov, *Siberian Acad Sci*, USSR
Dr. G.A. Eliseev, Kurchatov Institute, USSR
Dr. V.A. Glukhikh, Inst Electro-Physical, USSR
Institute Gen. Physics, USSR
Prof. T.J.M. Boyd, Univ College N Wales, WALES
Dr. K. Schindler, Ruhr Universitat, W. GERMANY
ASDEX Reading Rm, IPP/Max-Planck-Institut fur Plasmaphysik, F.R.G.
Nuclear Res Estab, Julich Ltd, W. GERMANY
Librarian, Max-Planck Institut, W. GERMANY
Bibliothek, Inst Plasmaforschung, W. GERMANY
Prof. R.K. Janev, Inst Phys, YUGOSLAVIA